Directivity pattern of flow-induced noise from a wall-mounted, finite length circular cylinder

Ric Porteous, Con J. Doolan and Danielle J. Moreau

School of Mechanical Eng. University of Adelaide, Adelaide, South Australia

ABSTRACT

Sound emanating from a wall-mounted, finite length cylinder immersed in cross flow presents a significant engineering problem and is relevant to a range of applications including aircraft landing gear and automobile appendages. However, despite its frequent occurrence in industry, there exists little experimental data on the noise created by such objects. To characterise this type of flow-induced noise source, acoustic directivity measurements have been taken in an anechoic wind tunnel at the University of Adelaide for wall-mounted cylinders of circular cross section. The aspect ratio (the cylinder length to diameter ratio, L/D) and orientation of the cylinders were varied to determine the influence of these parameters on noise directivity. Furthermore, the results were compared with the radiation pattern of the two dimensional case as well as with a dipole source (of equivalent power) at the assumed origin. The experimental data give further insight into the characteristics of the sound generated from wall-mounted, finite length cylinders in cross flow.

INTRODUCTION AND BACKGROUND

Flow-induced noise radiating from a slender cylindrical body is important to a range of applications including rail-pantographs, landing gear and automobile appendages.

Curle (1955) further developed Lighthill's acoustic analogy (Lighthill 1952) to include solid surfaces immersed in cross flow and related the radiated sound field to the fluctuating pressure on the surface. Phillips (1956) showed that for a circular cylinder in cross flow, this pressure is dominated by lift fluctuations at the vortex shedding frequency. Phillips (1956) developed Eq. 1 to describe the far field variation of mean square pressure, where ρ is the density, U is the free stream velocity, $St(=fD/U)$ is the Strouhal number of the fluctuating force based on the cylinder diameter, D, L is the cylinder length, s is the spanwise correlation length, x is the observer distance from the source, a_o is the speed of sound, $\overline{C_l^2}$ is the root mean square of the sectional lift coefficient and θ is the angle between the oncoming flow and the direction of the observer relative to the cylinder.

$$\overline{p^2} = \cos^2\theta \frac{\rho^2 U^6 St^2 \overline{C_l^2} Ls}{16a_o^2 x^2} \qquad (1)$$

Equation 1 shows that the directivity of the tone generated by the cylinder is dipole-like. Most studies on flow induced cylinder noise till present have focused on two dimensional cases (Ali et al. 2011; Cox 2008; Gerrard 1955) or quasi-3 dimensional cases (Fujita 2010; Schlinker 1976; Phillips 1956), where spanwise correlation of vortex shedding has been studied but three dimensional tip and junction (wall-cylinder interface) effects have not. In comparison, there are only a few studies related to noise from finite wall-mounted cylinders.

Becker et al. (2008) studied the flow field and flow induced noise from a square cylinder of length to diameter ratio of 6 at Reynolds numbers ranging from 1.3×10^5 to 3.8×10^5, in a turbulent boundary layer. Directivity measurements showed that acoustic radiation from the finite length cylinder at the vortex shedding frequency was dipole-like. Although one cylinder was studied comprehensively, cylinders with a range of aspect ratios and different cross sections were not.

King and Pfizenmaier (2009) studied sound produced by finite length cylinders of square, circular, rectangular and elliptical cross section, in a free jet at Reynolds numbers ranging from 4.1×10^4 to 8.8×10^4. Finite cylinders with aspect ratios ranging from 2 to 35 were tested. Higher aspect ratios were found to have a double peak in the acoustic spectra around the shedding frequency, which was attributed to tip effects. Acoustic spectra were presented but only for a measurement angle perpendicular to the cylinder plane.

Moreau and Doolan (2013) studied the influence of the aspect ratio of a finite length cylinder on radiated noise, taking into account both junction and tip effects. The noise spectra for both square and circular cross sectioned cylinders of aspect ratios ranging from 0.5 to 22.7 were measured at a single location at Reynolds numbers varying from 1.0×10^4 to 1.4×10^4. Additionally, unsteady wake velocity measurements were taken along the span of the cylinder and these velocity data were correlated with the acoustic measurements. It was found that at higher aspect ratios, both square and circular cylinders displayed multiple narrow band peaks in their acoustic spectra. This was attributed to cellular variation in the spanwise vortex shedding frequency that occurs due to flow around the free end and junction.

This paper will address the absence of data on the flow-induced noise of a wall-mounted finite cylinder by investigating the effect of systematically varying the aspect ratio, speed and cylinder orientation on the noise directivity.

EXPERIMENTAL SETUP

Anechoic wind tunnel facility

The experiment was conducted in the University of Adelaide's anechoic wind tunnel with internal dimensions of 1.4 m x 1.4 m x 1.6 m. The facility contains a rectangular contraction outlet with a height of 75 mm and a width of 275 mm. The wind tunnel walls are lined with foam wedges which provide an anechoic environment above 250 Hz. The maximum flow velocity of the free jet is approximately 35 m/s and the free stream turbulence is low at 0.33%.

Test models and mounting plate

A total of 16 test models were used. These included 15 circular cylinders with diameters of D=6 mm and aspect ratios (length to diameter ratio L/D) ranging from 0.8 to 22.7. The remaining model was a cylinder with a circular cross section that spanned the width of the contraction. The aspect ratio of this cylinder is denoted with the ∞ symbol.

The models were mounted, one by one, on a flat plate of length 300 mm and width 155 mm which, in turn, was attached to the contraction exit. To measure the directivity of the noise generated in orthogonal planes, the orientation of the cylinder was changed by attaching the plate to the top of the contraction, instead of changing the orientation of the microphone. This is shown in Figures 1 and 2 respectively. This was done because of spatial limitations inside the anechoic wind tunnel. Because of the small height of the contraction relative to its width, only the directivity of small aspect ratio cylinders were measured in the configuration shown in Fig. 2.

Careful consideration was given to aligning the plate flush with the exit plane so as not to disturb the boundary layer ahead of the cylinder. The centres of the cylinders were located 30 mm downstream of the contraction and were aligned with the centreline of the exit plane.

The full span cylinder was mounted on the contraction in a different manner to the finite cylinders. The mounting plate for the full span cylinder is the same as used by Moreau *et. al* (2011). It involves fixing the cylinder across the span without an endplate, so that the interaction between the wall boundary layer and root of the cylinder is replaced by an interaction with a free-shear layer. Essentially, the ends of the full span cylinder are located in a zero velocity environment. Fujita (2010) provides experimental evidence that the removal of end plates would lower the peak of any Aeolian tone observed due to increased velocity deficit in the wake and a decreased spanwise coherence of vortex shedding.

Equipment and method

Acoustic measurements were measured using a 4190 B&K ½'' microphone on a constant arc of radius R=515 mm from the centre of the cylinder at 11 different angular positions in the range from 30 to 107 degrees. This distance is one wavelength at 666 Hz, which indicates that any measurements above 666 Hz are valid far-field results. As will be shown, for some peaks, this lower limit is not always met. However, the geometric far field condition, R/D>1, is obtained in all cases.

The layout and coordinate system for measurements is illustrated in Figures 1 and 2. For a horizontally aligned cylinder (see Fig. 1), the plane of the measurement arc bisected the mid span of the measured cylinder. For a vertically orientated cylinder (see Fig. 2), the arc plane intersected the axis of the cylinder. To traverse the arc, the microphone was mounted on a Dantec automatic traverse with 6.25 μm positional accuracy. A wind sock was placed over the microphone to isolate it from low level recirculation inside the chamber. As stated in the transducer documentation, the error in sound pressure level measurements of the microphone is ±1 dB over its frequency response range (10-10,000 Hz).

Directivity measurements were taken at two different flow speeds of U_∞ =23 and 32 m/s. This corresponds to Reynolds
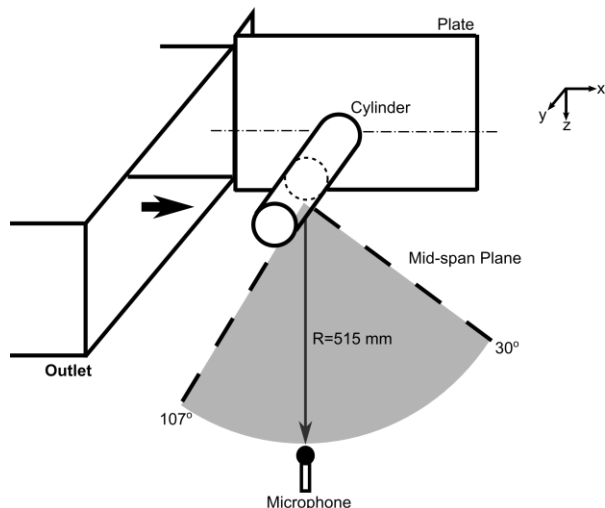
Figure 1: Experimental set up for the horizontally aligned cylinder (diagram not to scale).
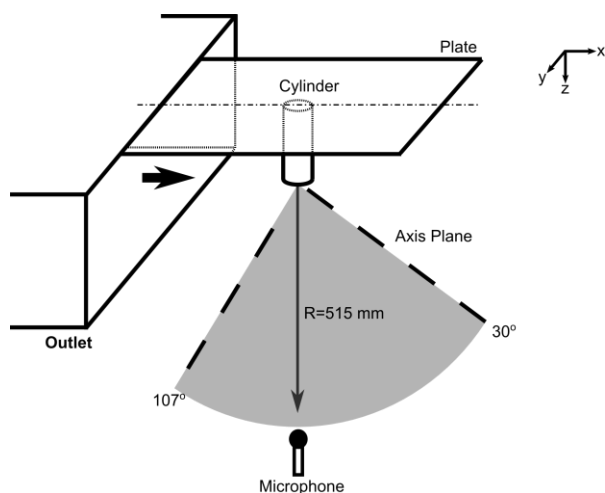
Figure 2: Experimental set up for the vertically aligned cylinder (diagram not to scale).

numbers (based on the diameter of the cylinder, Re_D) in the subcritical range of 8.7×10^3 for flow at 23 m/s and 1.2×10^4 for flow at 32 m/s which indicates that the wake is fully turbulent with laminar boundary layer separation on the periphery arc (Williamson 1996).

At each angular location, acoustic data were taken for 30 seconds at a sampling rate of 50 kHz. To create 1/3 octave band levels, a digital 1/3 octave band filter based on ANSI S1.11-1986 Order-3 filters was used. The frequency resolution of the narrow band power spectral density (PSD) was 0.033 Hz. The error in the PSD was calculated using inverse chi-squared method (Bendat and Peirsol 2012) resulting in an uncertainty of ±0.5 dB for a 95% confidence interval.

The blockage correction factor for the models using a very conservative value of drag coefficient of 2 was calculated to be approximately 0.7%. According to Becker *et al.*(2008) and Revell *et al.*(1977) this level of blockage error can be neglected in open circuit wind tunnels.

Contraction outlet flow conditions

Figures 3 and 4 shows the normalised velocity profile for the two different configurations. The velocity profiles closely

follow a 1/7th power law as shown. Table 1 shows the estimated boundary layer properties for the four cases. The results indicate that the boundary layer is in a fully turbulent state on the plate for both configurations at all flow speeds.
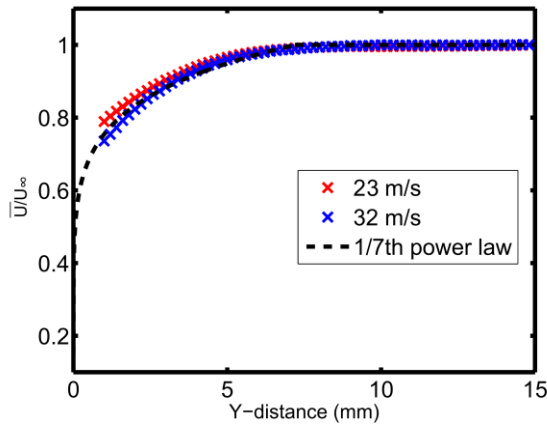
Figure 3: Boundary layer profile at the cylinder location in the horizontal orientation compared with 1/7th power law profile
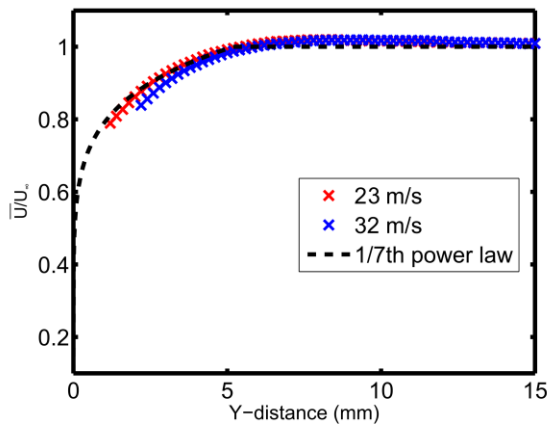
Figure 4: Boundary layer profile at the cylinder location in the vertical orientation compared with 1/7th power law profile

Table 1. Boundary layer characteristics

Orientation	Horizontal		Vertical	
	32 m/s	23 m/s	32 m/s	23 m/s
Boundary layer thickness, δ_{99} (mm)	13.4	10	5.4	5.8
Displacement thickness, δ^* (mm)	0.39	0.37	0.32	0.31
Momentum Thickness, θ (mm)	0.23	0.23	0.21	0.21
Shape Factor, H (=δ^*/θ)	1.69	1.63	1.52	1.51

Shear layer considerations

Sound emitted from an arbitrary source embedded in a uniform flow of finite width will experience refraction and attenuation or amplification upon crossing the shear layer. This effect is important to model when considering the radiative properties of a source in a uniform flow where the observer is in a quiescent environment, outside the mean flow, as in wind tunnel testing. Consequently, the data were corrected for shear layer effects using the shear layer correction equations derived by Amiet (1975). The general effect of the correction is to decrease the measured angle and increase the magnitude of pressure level at higher measurement angles. This results in an anti-clockwise rotation of the directivity pattern (in the coordinate system defined in Figs. 1 and 2) with a simultaneous upstream amplification.

It is important to note that these equations correct for the case where the uniform stream extends out to infinity. As such, the theoretical comparison based on the Lighthill-Curle analogy is not a simple $\cos^2 \theta$ relationship as in Equation 1, but that which has regard to the convective effects of mean flow, i.e the Doppler effect. This solution is obtained by solving the equations for a dipole in a mean flow based on the convective wave equation, as presented by Najafi-Yazdi *et al.* (2010). The normalised theoretical solution is shown as the saffron line in Figs. 7 through 12.

TEST CASES

Directivity measurements were taken for select aspect ratios, flow speeds and orientations, as summarised in Table 2.

Table 2. Summary of test cases

	Horizontal		Vertical	
L/D	32 m/s	23 m/s	32 m/s	23 m/s
∞	✓	✓		
22.7	✓	✓		
21.0	✓	✗		
19.3	✓	✗		
17.7	✓	✓		
16.0	✓	✗		
14.3	✓	✓		
12.8	✓	✗		
11.2	✓	✗	✓	✓
9.7	✓	✓	✓	✗
8.1	✓	✓	✓	✓
6.5	✓	✗	✓	✗
4.8	✓	✓	✓	✗
3.2	✓	✓	✓	✓
1.5	✓	✗	✓	✗
0.8	✓	✗	✓	✗

EXPERIMENTAL RESULTS

Acoustic spectra

Figures 5 and 6 show acoustic spectra for cylinders with selected aspect ratio at two different measurement angles, $\theta=90^o$ and $\theta=48^o$, for a flow speed of 32 m/s. The five cylinders chosen are representative of how the general behaviour of the acoustic spectra changes with aspect ratio. The background measurement was taken in the same manner as explained above but with the cylinder not present, i.e in the plane that would bisect the cylinder's midspan had it been there. Shown in Fig. 5 (in black) is the background measurement for a cylinder with L/D=22.7 only. It was noticed that background levels changed slightly with distance from the mounting plate, which explains why, in Fig. 5, the levels

decrease slightly below the indicated background level for smaller aspect ratio cylinders.

The full span cylinder (shown in red) has a single dominant peak at approximately 1021 Hz (St = 0.19), which corresponds to the vortex shedding frequency. Finite cylinders with L/D≥19.3 (shown in yellow) have a dominant double peak at the vortex shedding frequency. This double peak consist of a 'dominant' peak (at St = 0.19 for L/D=22.7) and a lower amplitude 'secondary dominant' peak at a lower frequency (at St = 0.18 for L/D = 22.7). The spectra also contains a 'secondary' (as opposed to 'secondary dominant') peak at approximately 400 Hz. Below an aspect ratio of L/D=19.3, the double tone becomes a single tone with decreased frequency (shown in green) and amplitude. At these aspect ratios, the secondary peak has constant amplitude. At L/D=9.7, the secondary peak is suppressed and only a weak tone at the shedding frequency is present, again at a lower frequency and amplitude (shown in blue). Below L/D=8.1, neither a dominant peak (single or double) or a secondary peak is present (shown in purple). Unlike that of the dominant vortex shedding peak, the secondary peak does not decrease in frequency or amplitude as the aspect ratio is changed. Moreau and Doolan (2013) provide evidence that suggests that multiple dominant peaks in the noise spectra are due to the cellular variation in spanwise vortex shedding frequency. The dominant peak is due to regular Karman vortex shedding at the midspan. The secondary dominant peak is due to a lower frequency shedding near the cylinder-wall junction owing to structures that form in the junction region interacting with the Karman vortex in the midspan. The secondary peak is associated with weak, low frequency shedding at the tip. This is attributed to suppression of vortex shedding at the tip due to the interaction of the downwash with regular Karman vortex shedding. Acoustic data for the finite aspect ratio cylinders at θ=90° agree with Moreau and Doolan's results, which gives confidence in the results at other angles.

The spectra at θ=48° in Fig. 6 shows that there is a directional dependence on the amplitude of the tonal components in the spectra. There is a simultaneous decrease in the secondary peak, dominant peak and secondary dominant peak amplitude with a decrease in observation angle.

Also shown in Figure 5 and 6 are the 1/3 octave band bounding frequencies (shown in as ticks under the bottom axis). The dominant peaks of cylinders with high aspect ratio (above 17.7) both fall within the same octave band. However, as the aspect ratio decreases further, because of the accompanying change in Strouhal number, the peak frequency of the lower aspect ratio cylinder falls within a different octave band than at higher aspect ratios. As such, it is not appropriate to calculate directivity patterns for these tones based on 1/3 octave centre band frequencies. Instead, the dominant and secondary dominant tonal directivities are evaluated at the frequency at which they occur. However, the secondary peak occurs at a relatively constant frequency (approximately 400 Hz) and the energy is spread around this centre frequency. It is difficult to locate an exact maxima for this tone. Consequently, 1/3 octave band levels were used to characterise this tonal component. This is an approach that was used by Becker *et. al* (2008) when measuring directivity around square cylinders.

Also apparent in the full span cylinder spectra in Figs. 5 and 6 are several tonal components in the range of 2 to 4 kHz. These are attributed to electromagnetic noise generated by surrounding instrumentation and harmonic overtones due to vortex shedding (each is annotated in the Figures). Electro-

magnetic noise does not appear in the spectra of finite aspect ratio cylinders because the BNC shielding was grounded during these measurements. Since the focus of this paper is on the components appearing in the range of 0.2 and 1 kHz, these additional components in the spectra are ignored.
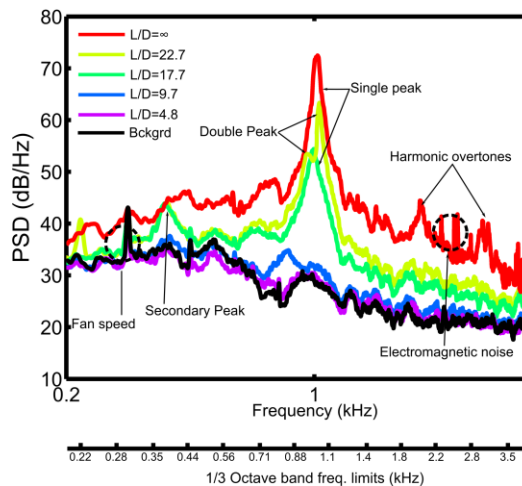
Figure 5: Comparison of Spectral density for cylinder L/D=∞, 22.7, 17.7, 9.7 and 4.8 at 90° measurement angle, with annotated points of interest
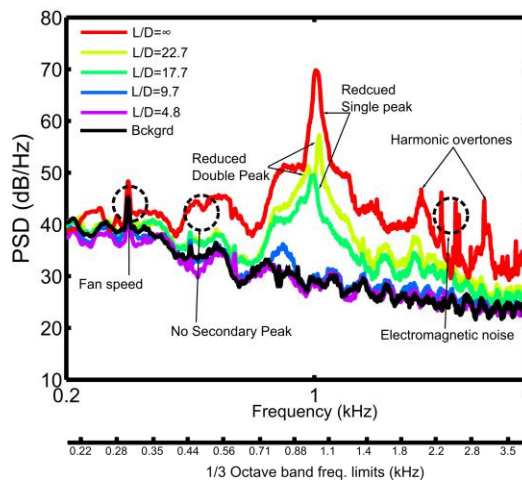
Figure 6: Comparison of Spectral density for cylinder L/D=∞, 22.7, 17.7, 9.7 and 4.8 at 48° measurement angle, with annotated points of interest

Directivity at 32 m/s

Figures 7 to 9 show the corrected directivity pattern for the three peak tones at a flow speed of 32 m/s. The cylinder aspect ratios for which these measurements are taken are indicated on the diagram. In all cases the data are normalised by the value associated with the highest aspect ratio measured at θ=90° measurement angle. The results are compared with the convective dipole solution in saffron.
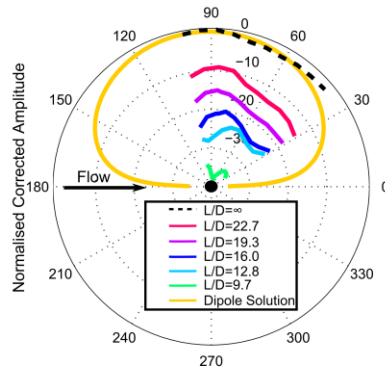
Figure 7: Directivity for the dominant tone at 32 m/s for select aspect ratio
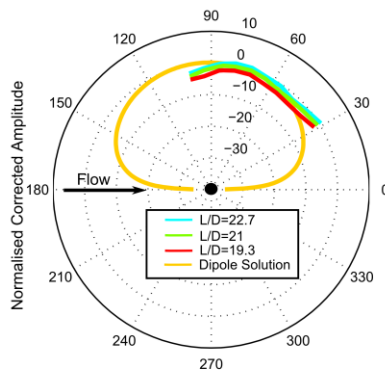
Figure 8: Directivity for the secondary dominant tone at 32 m/s for select aspect ratio
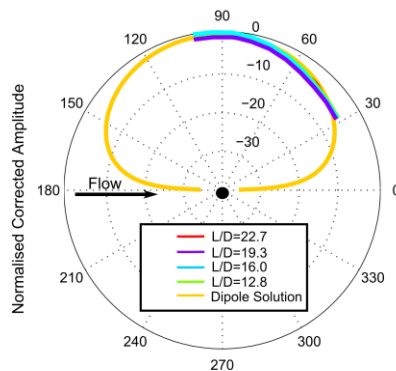
Figure 9: Directivity for the secondary tone at 32 m/s for select aspect ratio at 1/3 octave centre band frequency 400 Hz.

Figure 7 shows that for the dominant peak tone, there is a reasonable similarity between the theoretical and measured solution. The directivity is dipole-like and orientated perpendicular to the mean flow. The most salient feature of Fig. 7 is that the amplitude of the tone is decreased as the aspect ratio

decreases. What is also noticeable is that as the tone level gets closer to the background noise, the directivity becomes more quadrupole-like as indicated by the data for L/D=9.7.

Contrasting the results of Fig. 7 are Figs. 8 and 9, which show that there is a reasonable dipole-like directivity for the dominant secondary and secondary peak but no decrease in amplitude with changing aspect ratio. This is because the secondary dominant and secondary peaks are attributed to root and tip flow structures respectively, while the dominant peak is associated with midspan vortex shedding (Moreau and Doolan 2013). From Eq. (1), as the length of the cylinder decreases, so too does the amplitude of the tone. However, the root and tip of the cylinder remain geometrically constant regardless of the aspect ratio, which explains the invariant nature of these noise components. The dipole-like nature of the tone indicates that the unsteady forces producing this component of the spectra are perpendicular to the mean flow.

Directivity at 23 m/s

The aspect ratios at which dominant and secondary peaks occur at 32 m/s also display dominant and secondary peaks at 23 m/s. The only substantial difference is that the amplitude of the peaks are reduced. Schlinker and Fink (1976) and Phillips (1956) have shown that amplitude of the peaks scale with the 6th power of flow velocity. The directivity of the three tones in the noise spectra (at aspect ratios where they occur) is shown in Figs. 10 through 12. The data in Fig. 10 is normalised by that of the full span cylinder at 23 m/s, while results of Figs. 11 and 12 are normalised against the value of the highest aspect ratio displayed at the 90° measurement angle.

As shown in Fig. 10 and 11, the characteristics of the dominant and secondary tones remain largely unchanged with decreasing mean flow velocity. The directional characteristics are, again, dipole-like. This is to be expected when considering the flow regime the cylinder is operating in. Williamson (1996) outlines that the flow over cylinders is dynamically similar in Reynolds numbers ranging from 1×10^{3} to 2×10^{5}. Phillips (1956) invokes Reynolds number similarity arguments to lend support to the 6th power velocity collapse within dynamically similar flow regimes. Hence it is reasonable to also expect a similar directional characteristic of the peak tones within this Reynolds number region.

In contrast, the directivity of the secondary tone shows substantial disparity when compared with results of higher velocities (Fig. 9). The amplitude of the tone seems to be independent of the aspect ratio, however the directional characteristics are more akin to a dipole rotated 90°. It should be noted, however, that at these flow speeds the peak is very wide in the spectra. Taking 1/3 octave bands around the peak frequency may be including additional turbulent energy which would augment the directional characteristics of the tone. It should also be noted that measurements at 250 Hz are well below the threshold of the acoustic far field. Nevertheless, further investigation is required to explain the disparity.
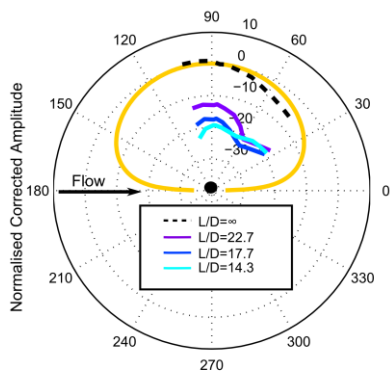
Figure 10: Directivity for the peak tone at 23 m/s for select aspect ratio
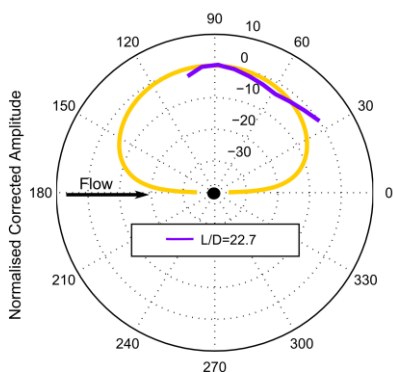
Figure 11: Directivity for the secondary dominant tone at 23 m/s for select aspect ratio
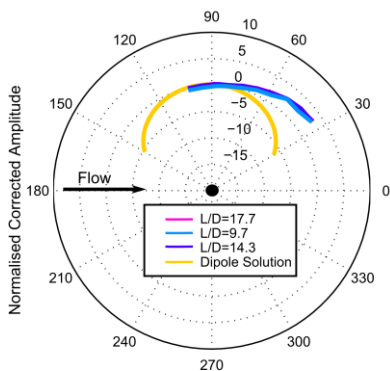
Figure 12: Directivity for the secondary tone at 23 m/s for select aspect ratio at 1/3 octave centre band frequency 250 Hz.

Effect of changing the orientation

Spectra for cylinders with selected aspect ratio in the vertical orientation were taken. New background measurements were taken to account for the changed position of the plate relative

to the microphone. There was no difference in background and measured acoustic data when the cylinder was orientated vertically and hence the results are not shown. The limit of the cylinder aspect ratios which could be tested in this orientation exactly coincided with the disappearance of all peaks in the spectra.

To further investigate the effect of orientation, the cylinders were mounted in the horizontal configuration (Fig. 1) and microphone measurements were made at 515 mm from the centre of the cylinder along the cylinder axis. This was done using a microphone stand instead of the traverse. Because of the impracticalities of using a microphone stand, only a single measurement angle was recorded.

Figure 13 shows the spectra associated with the higher aspect ratio cylinders in a vertical orientation at $\theta=90^{o}$ and a comparison is made with the background measurement.

The results indicate that there is still the existence of the dominant peak and, in the case of the highest aspect ratio cylinder, a secondary dominant peak. Comparison with Figure 4 indicates that the amplitude of the both dominant and secondary dominant peak is significantly reduced. Figures 7 through 9 shows that these components are dipole in nature with the axis normal to the mean flow and hence it is expected to have much reduced amplitude in a position along the axis of the cylinder.
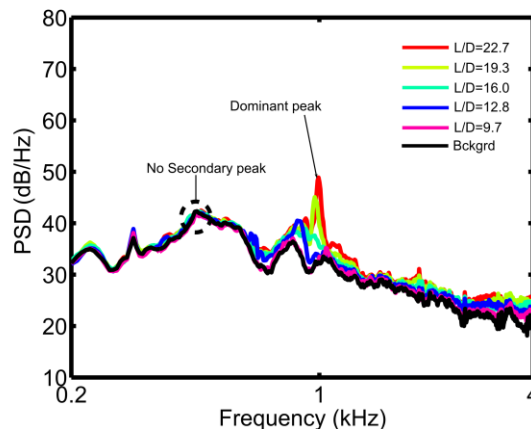
Figure 13: Spectra for select higher aspect ratio in the horizontal orientation along the cylinder axis at 32 m/s

Notable here is the complete absence of the secondary tone for any cylinder. This result is surprising as it would be expected that at least some remanent of the low frequency tip tone would occur in an orientation along the cylinder axis.

COMMENT ON RESULTS OF KING AND PFIZINMAIER (2009)

Because of the scarcity of acoustic data on finite length cylinders, it is important to correlate results with the work of others and explain any differences. Significant comparison with the work of Moreau and Doolan (2013) has been made throughout this paper and are shown to compare favourably. King and Pfizinmaier (2009) are the only other authors to have studied tip flow effects on noise spectra of circular cylinders. They also found a secondary dominant peak at higher aspect ratio cylinders in addition to the dominant vortex shedding peak. However, there exists an interesting disparity between the interpretation by King and Pfizinmaier (2009)

and Moreau and Doolan (2013) about the origin of the secondary dominant peak. King and Pfizinmaier attribute the secondary dominant peak to tip effects, without substantial explanation. Moreau and Doolan suggest that the secondary dominant peak in the spectra originates from a lower vortex shedding frequency at the root based on correlation of acoustic and velocity spectra. Junction effects could not have caused King and Pfizinmaier's results as they eliminated the cylinder-wall junction from their experiment by placing outside of the mean flow. The results in this study lend support to that of Moreau and Doolan's, specifically that tip flow structures are responsible for the very low frequency Aeolian tone, while junction effects are responsible for the secondary dominant peak near the vortex shedding frequency. A possible explanation is that King and Pfizinmaier studied flow over the tip of much larger cylinders which produced tones at lower frequencies. The reported secondary dominant peak may be a manifestation of the low frequency secondary peak associated with the tip, which happens to be near to the vortex shedding frequency. This would give the appearance of a double peak. Alternatively, the placement of the cylinder in a free shear layer may induce somewhat similar behaviour to being immersed in a wall boundary layer. It is unclear whether the results given by King and Pfizinmaier show that the secondary peak is invariant to aspect ratio, which would lend more support to the aforementioned hypotheses.

CONCLUSIONS

This study has investigated the effect of changing aspect ratio on the directional characteristic of the tones produced by a finite wall-mounted circular cylinder. The acoustic spectra of such bodies were found to have three main peaks attributed to the midspan ('dominant' peak), the base ('secondary dominant' peak) and tip ('secondary peak') flow structures in previous work. Cylinders of aspect ratios ranging from 0.8 to 22.7 for two different velocities and orientations were measured. The results were compared with that of a full span cylinder and the solution for a dipole source in a mean flow. The main conclusions to be drawn from this study are:

- The directional characteristic of the dominant peak are mostly dipole-like, with the amplitude decreasing as aspect ratio decreases.
- The directional characteristics of the secondary dominant and secondary peaks are dipole-like, but with amplitudes that do not change with aspect ratio. These results are attributed to the fact that the geometry of the tip and root of the cylinder as well as the boundary layer height remain unchanged with the changing aspect ratio.
- A change in velocity does not change the directivity of the dominant peaks. This is to be expected as the test Reynolds number indicates that the cylinders are operating in similar vortex shedding regimes. Changing the velocity has a substantial effect on the directivity of the secondary peak.
- Changing the orientation of the cylinder has a significant effect on the directivity. For lower aspect ratio cylinders, a vertically aligned cylinder is no different to background noise levels. However, for higher aspect ratio cylinders, preliminary results indicate that the dominant single peak and secondary peak are significantly reduced. The secondary peak is absent from the measured spectra.

REFERENCES

Ali, M.S.M & Doolan, C.J & Wheatley, V (2011), *'The sound generated by a square cylinder with a splitter plate at low Reynolds Number'*, Journal of Sound and Vibration, Vol. 330, pp. 3620-3635

Amiet, R.K (1975), *'Correction of open jet wind tunnel meas-urements for shear layer refraction'*, AIAA 2nd Aeroacoustics conference, Hampton,V.A

Becker, S & Hahn, C & Kaltenbacher, M & Lerch, R (2008), *'Flow-Induced Sound of Wall-Mounted Cylinders with Different Geometries'*, AIAA Journal, Vol. 46, 2256-2281

Bendot, J.S & Peirsol, A.G (2012) *'Random Data Analysis and Measurement Procedures'*, 4th Edition, John Wiley & Sons, Hoboken, New Jersey

Cox, J. S (1998), *'Computation of Vortex Shedding and Radiated Sound for a Circular Cylinder: Subcritical to Transcritial Reynolds Numbers'*, Theoretical Computational Fluid Dynamics, Vol. 12, pp. 233-253

Curle, N (1955), *'The Influence of Solid Boundaries upon Aerodynamic Sound'*, Proceedings of the Royal Society of London. Series A, Mathematical and Physical Sciences, Vol. 231, pp. 505-514

Fujita, H (2010), *'The characteristics of the Aeolian tone radi-ated from two-dimensional cylinders'*, Fluid Dynamics Research, Vol. 42, pp. 1-25.

Gerrard, J. H (1955), *'Measurements of the sound from a circular cylinders in an airstream'*, Proceedings of the Royal Society of London, Series B, Vol. 68, pp. 453-461

King, W.F & Pfizenmaier, E (2009), *'An experimental study of sound generated by flows around cylinders of different cross-section'*, Journal of Sound and Vibration, Vol. 328, pp. 318-337

Lighthill, M.J (1952), *'On sound generated aerodynamically'*, Proceedings of the Royal Society of London. Series A, Mathematical and Physical Sciences, Vol. 211, pp. 564-587

Moreau, D.J & Brooks, L.A & Doolan, C.J (2011) *'Broadband trailing edge noise from a sharp-edged strut'*, The Journal of the Acoustical Society of America, Vol, 129,pp. 2820

Moreau, D.J. and Doolan, C.J (2013), *'Flow-induced sound of wall-mounted finite length cylinders'*, AIAA Journal, accessed 7 August, 2013. doi: 10.2514/1.J052391 <http://arc.aiaa.org/doi/abs/10.2514/1.J052391>

Najafi-Yazdi, A & Bres, G.A, & Mongeau, L (2010), *'An acoustics analogy formulation for moving sources in uniformly moving media'*, Proceedings of the Royal Society of London. Series A, Mathematical, Physical and Engineering Sciences, Vol. 467, pp. 144-165

Phillips, O.M (1956), *'The intensity of Aeolian Tones'*, Journal of Fluid Mechanics, Vol. 1, pp. 607-624

Revell, J.D & Prydz, R.A & Hays, A.P (1978), *'Experimental Study of Aerodynamic Noise vs Drag Relationships for Circular Cylinders'*, AIAA Journal, Vol. 16, pp. 889-897

Schlinker, R. H & Fink, M. R. (1976) *'Vortex noise form non-rotating cylinders and airfoils'*, AIAA 14th Aerospace Sciences meeting, Washington D.C

Williamson, C. H. K (1996) *'Vortex Dynamics in the Cylinder Wake'*, Annual Reviews of Fluid Mechanics, Vol. 28, pp. 477-539